

C–H···O Non-Classical Hydrogen Bonding in the Stereomechanics of Organic Transformations: Theory and Recognition

Ryne C. Johnston, Paul Ha-Yeon Cheong*

Received (in XXX, XXX) Xth XXXXXXXXXX 20XX, Accepted Xth XXXXXXXXXX 20XX

DOI: 10.1039/b000000x

This manuscript describes the role of non-classical hydrogen bonds (NCHBs), specifically C–H···O interactions, in modern synthetic organic transformations. Our goal is to point out the seminal examples where C–H···O interactions have been invoked as a key stereocontrolling element and to provide predictive value in recognizing future and/or potential C–H···O interactions in modern transformations.

1 Introduction

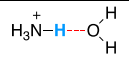
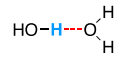
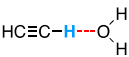
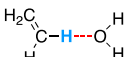
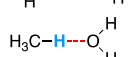
Hydrogen (X–H···A) bonding^{1,2} is central to chemistry³ and biology.⁴ Exemplified in water networks⁵ and peptide interactions,⁶ classical hydrogen bonding involves highly polar donors in the presence of strongly electronegative acceptors (X = A = N, O, F). A number of early reports in the 1930s described anomalous properties of molecules like HCN⁷ and acetyl chloride^{4a} exhibiting hydrogen bonding behaviour while having no traditional X–H donor. These studies also showed that less electronegative C–H bonds could be donors as well as other lone-pair bearing atoms and functional groups (sulfur, phosphorous and various π -systems) could be suitable acceptors. Many detailed crystallographic analyses of both inorganic and organic systems in the 1950s and 1960s revealed close C–H···O/N contacts, evidencing the stabilization afforded by “non-classical” hydrogen bonds (NCHBs).⁸ NCHBs are also found in biological systems; an example being the thiamine-adenine base pair interaction in RNA.⁹ These NCHBs, while weaker ($\Delta G_{\text{interaction}} = -0.5$ to -3.7 kcal/mol)¹⁰ than classical hydrogen bonds ($\Delta G_{\text{interaction}} = -3.1$ to -6.9 kcal/mol),¹¹ are still found to provide enough stabilization to render complete control of selectivity in chemical reactions.¹²

2 General Properties of C–H···O interactions

C–H···O interactions are distinct from van der Waals interactions¹³ — H···O distances in C–H···O interactions are often shorter than the sum of the van der Waals radii (2.7 Å for O and H). They also often display directionality (i.e., linear bonds are more stable than bent), indicative of orbital interactions.¹⁴

Desiraju postulated that NCHBs are a subset of hydrogen bonding.^{6c} Indeed, the strength of the H···O interaction, classical or otherwise, is proportional to the polarization of the donor C–H and the charge of the acceptor heteroatom; i.e., more acidic hydrogens and greater anionic characters in acceptors result in stronger hydrogen bonds. As shown in Table 1, the trend of proton acidity with respect to hybridization decreases as follows: $sp > sp^2 > sp^3$.^{15,16}

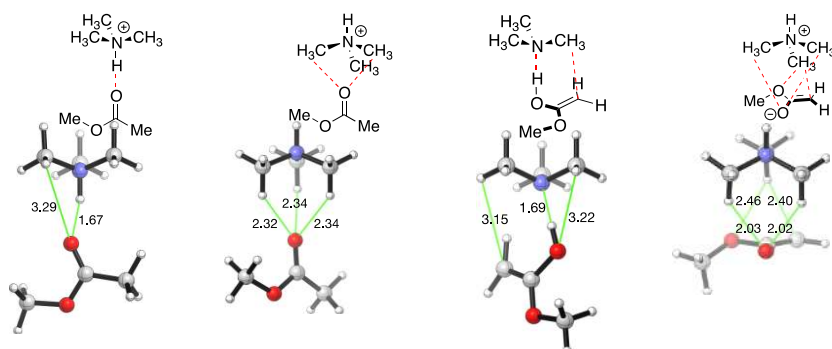
Table 1 Gas-phase distances and energies (ΔH) of salient hydrogen bonding dimers. Distances are in Å, and energies in kcal/mol.[‡]

Dimer	H···O Distance	Energy (ΔH)	Ref.
	1.74	19	16a
	1.96	4.7	14a
	2.17	2.5	16b
	2.38	0.9	16b
	2.51	0.3	14a

[‡]See original literature for computational details.

Direct experimental observation of transition state NCHBs is difficult because of the short lifespan (< 200 fs) of TSs.¹⁷ However, NCHBs in the ground state have been documented via infrared and NMR spectroscopy. C–H···O interactions are characterized in the IR by a strong redshift ($-40 \text{ cm}^{-1} > \Delta\nu > -80 \text{ cm}^{-1}$) for alkynes, little to no redshift ($0 \text{ cm}^{-1} > \Delta\nu > -20 \text{ cm}^{-1}$) for alkenes, and a medium blueshift ($+60 \text{ cm}^{-1} > \Delta\nu > +10 \text{ cm}^{-1}$) for alkanes. Redshifted (lengthened) C–H bonds, typically seen in classical hydrogen bonding, result from lone pair donation of acceptor A into the σ^* C–H, the extreme of which is full deprotonation. Conversely, a blueshift (contraction) results when an electron-deficient R_3C-H bond, already lengthened, is compressed by electron density donation from an electron-rich A.^{16b,18} ¹H-NMR observation is typically marked by an upfield shift of the proton of interest depending on the strength of the hydrogen bond. Alkynes are characterized by a 1.9 ppm shift upfield, alkenes by a 1.5 ppm shift, and alkanes by a 1.2 ppm shift.^{13,19}

Table 2 Binding energies (ΔZPE) of complexes of trimethylammonium with methyl acrylate. Solid green lines show electrostatic interactions. Computations performed at MP2/6-311++G**, with interaction free energies given in kcal/mol



Solvent	$N^+-H\cdots O_{\text{carbonyl}}$	$C(sp^3)-H\cdots O_{\text{carbonyl}}$	$N\cdots H-O_{\text{enol}}$	$C(sp^3)-H\cdots O_{\text{enolate}/\pi}$	ϵ_r
gas	-19.7	-12.9	-10.9	-95.1	1.0
PhMe	-10.3	-5.2	-8.1	-40.9	2.4
$CHCl_3$	-7.5	-3.4	-7.8	-22.2	4.7
THF	-6.2	-2.2	-7.2	-15.2	7.6
MeOH	+0.3	+2.0	-4.3	+0.7	32.7
H_2O	+0.8	+2.4	-3.9	+2.3	80.1

3 C–H \cdots O Interactions in Synthesis

E. J. Corey popularized NCHBs in transition states (TSs). He extended the idea of stabilizing C–H \cdots O interactions to TS geometries, recognizing their potential roles in both rigidifying the TS (preorganization) and in overcoming the entropic cost of preorganization.²⁰ Selectivity by NCHBs arise in two ways: 1) where NCHB stabilization is only possible in the major TS, and 2) where NCHB interactions exist in all TSs, but the resultant preorganization forces the minor TSs to incur destabilizing steric and/or electrostatic interactions.

Various archetypical stereoselective transformations²¹ controlled by NCHBs are discussed in the following sections, organized by the type of C–H donors. While C(sp) \cdots H donors are expected to be the strongest, there have been no reports to date implicating the alkynyl proton as a stereocontrolling element.

The enhanced basicity of the imine nitrogen is such that

3.1 C(sp³)–H donors

C(sp³)–H donors can be subdivided into activated and unactivated donors. Activated donors are α to a full or developing positive charge, and are most commonly seen in pnictogen- and metal-bearing molecules. Examples involving unactivated donors are fewer, and mostly involve distal methyl or methylene groups at a critical point. In both cases, proximity to an electron-withdrawing group increases the C–H donating ability.

3.1.1 Activated C(sp³)–H donors

3.1.1.1 Ammonium $N^+-C(sp^3)-H\cdots O$ interactions

In 2002, Houk reported the magnitude of HB and NCHB stabilizations between trimethylammonium with methyl acetate or the methyl acetate enolate (Table 2).²² In all cases, the magnitudes of classical hydrogen bonding interactions were greater than those of the NCHB interactions. It was also shown that solvent environment had a dramatic effect on the magnitude of stabilization – these interactions are the strongest in the gas phase and non-polar solvents, and decreases as the solvent polarity increases.²³

The greatest interaction is experienced in the tight ion pair of

the trimethylammonium $N^+-C(sp^3)-H$ complexing to the negatively charged enolate oxygen and the π -system, resulting in a dramatic 95 kcal/mol of stabilization in the gas phase. The C(sp³)–H \cdots O distances are also remarkably short (2.02 Å). Conversely, the weakest interaction is the post-proton transfer complex of the enol and the deprotonated ammonium ($N\cdots H-O$), at only 10.9 kcal/mol stabilization.

Comparisons of the neutral acceptor, methyl acetate, illustrate the relative strengths of classical and non-classical hydrogen bonding. The stabilization afforded by three NCHB interactions ($N^+-C(sp^3)-H\cdots O_{\text{carbonyl}}$) amounts to about two-thirds the stabilization of a single classical hydrogen bond ($N^+-H\cdots O_{\text{carbonyl}}$) (-12.9 kcal/mol and -19.7 kcal/mol, respectively).

These specific model systems and interactions are integral to understanding *cinchona* catalysis, and have since been employed to describe the enantiocontrol in a number of reactions.²⁴

3.1.1.2 Iminium $N^+-C(sp^3)-H\cdots O$ interactions

Houk reported the mechanism and origins of stereoselectivity of the Hajos-Parrish reaction²⁵ (Figure 1).²⁶ C–H \cdots O interactions were seen to be important in controlling the stereoselectivity in the aldol and Mannich reactions. The stereoselectivity in the Hajos-Parrish arises from the addition of the proline-enamine to one of two cyclic ketones. The enantioselectivity originates primarily from the greater iminium planarity distortion in the *syn*-enamine **TS-(R,R)** compared to the *anti* **TS-(S,S)**. A secondary stereocontrolling factor is the ability of a prolinyl C(sp³)–H to stabilize the developing negative charge on the carbonyl oxygen (shown in green lines in Figure 1) — the major **TS-(S,S)** exhibits a shorter C–H \cdots O interaction and is lower in energy by 3.4 kcal/mol than **TS-(R,R)**, where this interaction is more distal and presumably weaker.

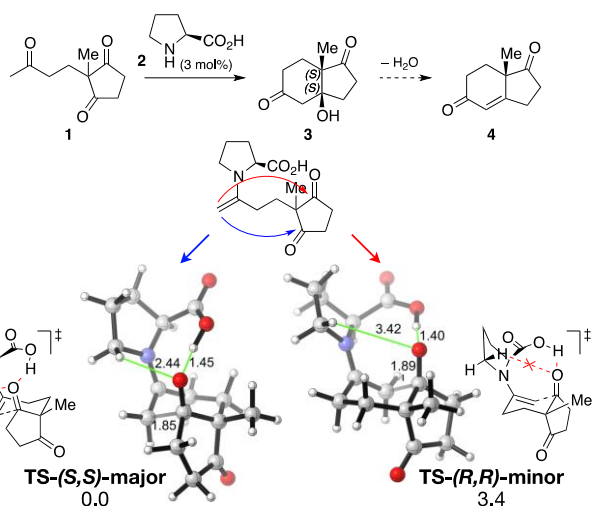


Figure 1 Houk's model for the enantiocontrol in the Hajos-Parrish reaction. Enamine planarity and NCHB with the proline α -methylene hydrogens control selectivity for **TS-(S,S)**. Solid green lines show electrostatic interactions, grey lines show forming bonds. Computations performed at B3LYP/6-31G*, with free energies given in kcal/mol.

3.1.2. Unactivated $C(sp^3)$ -H donors

3.1.2.1 Allylic- $C(sp^3)$ -H...O interactions

Sordo reported a computational study of the *meta/para* selectivity in the hetero [4+2] between SO_2 and isoprene in 1994. To our knowledge, this is the earliest work citing NCHBs as selectivity controlling elements in the TS (Figure 2).^{27,28} He showed that sultine regioselectivity is controlled by the $C(sp^3)$ -H...O NCHB interaction between the sulfonyl oxygen and the isoprene methyl. **TS-*meta-endo***, with the $C(sp^3)$ -H...O interaction, is 1.8 kcal/mol more stable than **TS-*para-endo***, where this interaction is absent. As shown by the *para-endo* and *para-exo* TSs, the *endo* preference²⁹ in this reaction is minimal (0.2 kcal/mol).

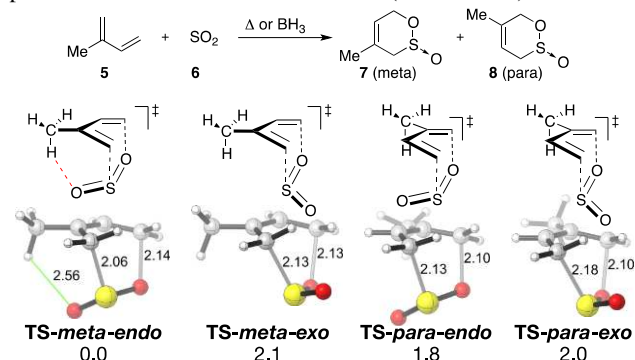


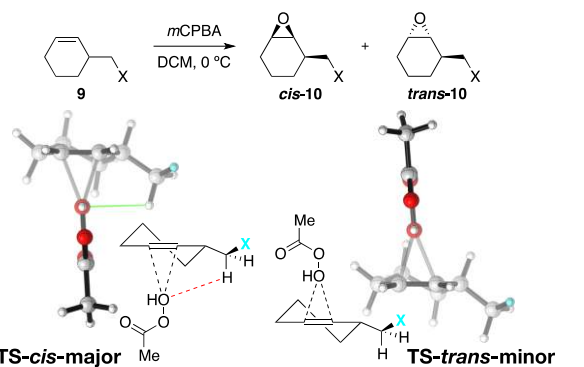
Figure 2 SO_2 regioselectively adds to isoprene in the **TS-*meta-endo*** fashion to engage in NCHB. Solid green lines show electrostatic interactions, while grey lines show forming bonds. Computations performed at MP2/6-31G**/HF/6-31G*, with interaction free energies given in kcal/mol.

3.1.2.2 Alkyl- $C(sp^3)$ -H...O interactions

In 2001, Houk reported the role of unactivated $C(sp^3)$ -H donors in controlling the stereoselectivity of epoxidations.³⁰ The origin of π -facial selectivity comes from the propensity of the peracid to approach from the face where an NCHB with the terminal peracid oxygen and the C3 α -hydrogens may be realized (Table 3). Furthermore, the selectivity afforded by these NCHBs

is enhanced as the electron-withdrawing ability of the C3 α -substituent increases – the *cis* preference increases from 0.2 kcal/mol (exp.: 1:1 *cis:trans*) in the hydrogen case to 2.3 kcal/mol (exp.: 13:1 *cis:trans*) in the mesylate.

Table 3 Approach from the π -face where NCHBs are present is preferred. π -Facial selectivity of peracid epoxidation increases with the electron-withdrawing ability of X. Solid green lines show electrostatic interactions, while grey lines show forming bonds. Computations performed at B3LYP/6-31+G**/B3LYP/6-31G*, with interaction free energies given in kcal/mol.



X	<i>cis:trans</i> (exp.)	$\Delta\Delta E_{trans-cis}$ (exp.)	$\Delta\Delta E_{trans-cis}$ (comp.)
H	1:1	0.0	0.2
Br	2.3:1	0.4	1.7
CN	4:1	0.8	1.5
OMs	13.3:1	1.4	2.3

3.2 $C(sp^2)$ -H donors

NCHB involving $C(sp^2)$ -H are often strong, and can impart preorganization of the TS. By far, the most common of this type are formyl groups. The ubiquity of formyl groups in many highly stereoselective allylboration, aldol and Diels-Alder reactions is conspicuous. The origin of this phenomenon is the presence of NCHB involving the formyl hydrogen that contributes to heightened stereocontrol. Imine C-H donors have similarly been shown to engage in NCHB.³¹

3.2.1. Ground and transition state stabilization

In 1997, Corey proposed stereochemical models governing the enantioselectivity of aldol reactions utilizing oxazaborolidine Lewis acids (Figure 3).^{20b-d,32} He invoked a two-point binding motif in the ground state catalyst-aldehyde complex, which is preserved through the transition state. The primary binding arises from the substrate carbonyl-boron dative bond. The second arises from a NCHB between the formyl hydrogen and the oxazaborolidine oxygen. This two-point binding motif, when coupled with the catalysts' chiral substituents, imparts facial control of addition to the aldehyde. While initial computational studies³³ found this motif to be less favourable, more recent studies³⁴ have upheld Corey's proposal.

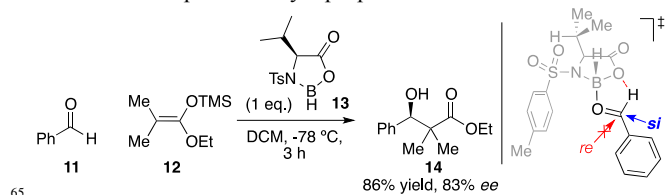


Figure 3 Corey's oxazaborolidine-catalyzed Mukaiyama aldol (left). Proposed stereochemical model (right) showing two-point binding, with the catalyst tosyl group shielding the *re*-face.

The related oxazaborolidinium catalysts have also been applied to Diels-Alder reactions (Figure 4, top left).³⁵ Like the aldol, the dienophile is bound to the catalyst primarily by the carbonyl oxygen-boron dative bond, and secondarily by NCHB between the formyl proton and the oxazaborolidinium oxygen.

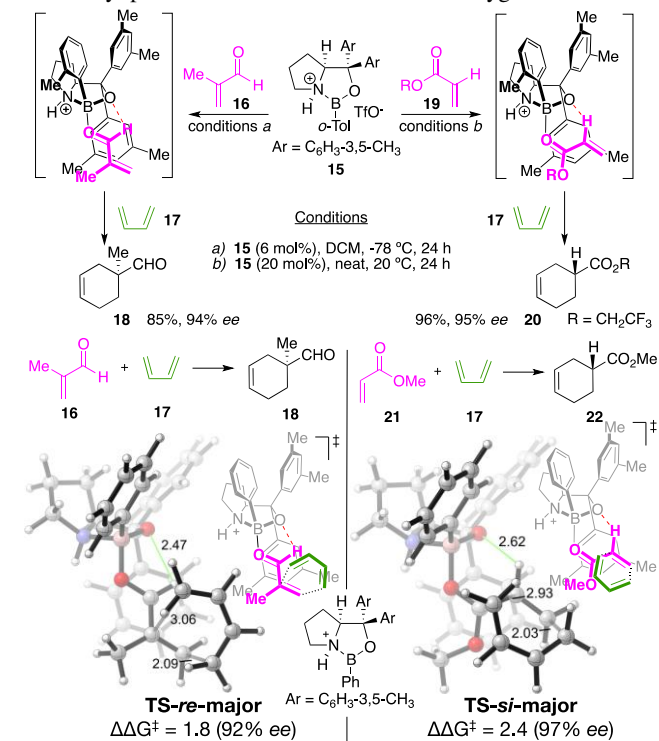


Figure 4 Corey's oxazaborolidinium **15** catalyzed Diels-Alder cycloaddition of vinyllogous aldehydes (left) and esters (right) with 1,3-butadiene, and their respective proposed catalyst-substrate complexes. The catalyst aryl group blocks the concave face of the substrate. Houk's computational investigation on Corey's oxazaborolidinium-catalyzed [4+2]-cycloaddition with methacrylaldehyde (left) and methyl acrylate (right). The catalyst aryl group blocks the concave face of the substrate. Solid green lines show electrostatic interactions, while grey lines show forming bonds. Computations performed at B3LYP/6-31G*/PCM(DCM)//B3LYP/6-31G*, with interaction free energies given in kcal/mol.

In 2009, Houk verified these models computationally using a slightly simplified catalyst involving a Ph, rather than *o*-Tol on the borane (Figure 4, bottom left).³⁶ The two point binding provided by the dative B–O bond and the C–H⋯O NCHB interaction restrict dienophile rotation, and allows for the facial discrimination. Steric occlusion by the downward-facing oxazaborolidinium aryl group prevents *si*-addition, which leads to the minor product.

In 2002, Corey reported that these oxazaborolidinium catalysts also perform well with acrylates and fumarates (Figure 4, top right).^{35b-d} In the absence of a formyl hydrogen, an NCHB with the vinyllogous hydrogen acts as secondary binding, rigidifying the transition state. Houk verified this vinyllogous C(sp²)–H⋯O interaction in α,β-unsaturated carbonyl compounds, citing the same stereocontrol model as in the formyl cases (Figure 4, bottom right).³⁶

3.2.2. Transition state stabilization

Transient NCHBs found only in the transition state can also induce high selectivity.

In 1998, Paterson applied the formyl C–H⋯O NCHB model to explain the 1,4-*syn* stereoselection in the boron-mediated aldol addition of aldehydes to α-alkoxy ketones **15** (Figure 5).³⁷ This featured repeatedly in the synthesis of polyketide ACRL Toxin IIIB to create C₈–C₉ and C₁₂–C₁₃ linkages. The chair TS, featuring a C–H⋯O interaction between a benzoyl carbonyl oxygen and a formyl hydrogen, leads to the major 1,4-*syn* product. In the TS leading to the minor 1,4-*anti* product, the chair flip replaces the stabilizing C–H⋯O interaction with a repulsive alkyl:alkyl steric repulsion between the β-methyl and the axial boron ligand.

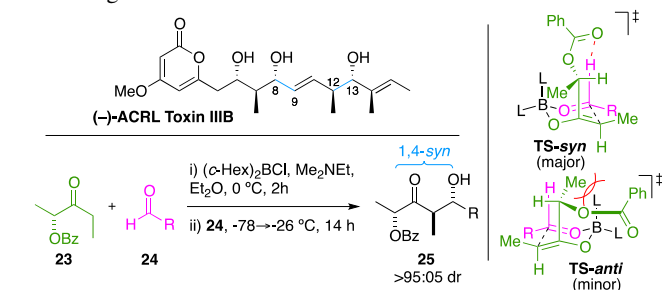


Figure 5 ACRL Toxin IIIB (top). 1,4-*syn* selective boron-aldol (bottom). Proposed stereochemical model (right) showing critical formyl C(sp²)–H⋯O interaction in the favoured TS, while steric repulsion destabilizes the disfavoured TS.

Goodman later investigated the origins of a related 1,5-stereoselection in a number of alkoxy and acetal-protected β-alkoxy and β-THP ketones (Figure 6).³⁸ Computations revealed a significant stabilizing C(sp²)–H⋯O interaction in a boat conformation.³⁹ The critical NCHB results from the proximity of the axial alkoxy oxygen to the axial formyl hydrogen, in a seven-membered ring. Like in Paterson's report, Goodman's model derives the selectivity from the chirality of the β-alkoxy center: In order to maintain the NCHB stabilization, the minor **TS-in-syn** incurs steric repulsion with the bulky β-R group, amounting to 0.3 kcal/mol selectivity.

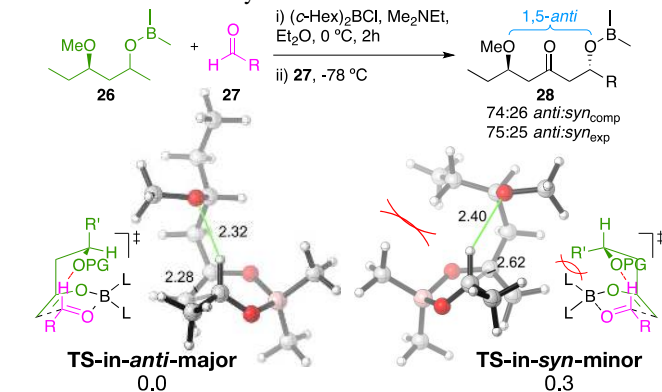


Figure 6 Goodman's rationalization for the 1,5-*anti* boron-aldol. Solid green lines show electrostatic interactions, while grey lines show forming bonds. Computations performed at B3LYP/6-31G*/PCM(Et₂O)//B3LYP/6-31G**, with interaction free energies given in kcal/mol.

Antilla reported in 2010 the enantioselective allylboration of aldehydes catalyzed by chiral phosphoric acid (CPA) (Figure 7).⁴⁰ He proposed a chairlike structure as a likely TS, invoking classical hydrogen bond activation of the equatorial boronate oxygen by the CPA proton.⁴¹

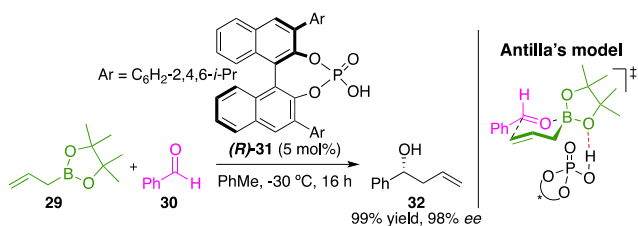


Figure 7 Antilla's stereochemical model (*right*) for the enantioselective allylboration catalyzed by chiral phosphoric acid **23** (*left*) classically hydrogen bonding to pinacol ligand.

5 Goodman reported a computational study examining the enantiocontrol in this reaction (Figure 8).⁴² He found that the CPA acts as a bidentate hydrogen bonding ligand, complexing the axial boronate oxygen by classical hydrogen bond (O–H···O) and the aldehyde through NCHB between the formyl hydrogen and the phosphoryl oxygen (C–H···O=P). This two point-binding motif by the CPA conformationally locks the chair transition states and allows for enantiocontrol by the chiral groups on the CPA. The steric clash of the boronate and the CPA aryl group in the minor **TS-*si*** amounts to 6.1 kcal/mol of selectivity. Goodman also found that the Antilla TS is 8.2 kcal/mol higher and results in poorer selectivity ($\Delta\Delta G^\ddagger = 1.6$ kcal/mol). The importance of C–H···O interactions in these reactions have also been shown in recent reports by Houk and Antilla.⁴³

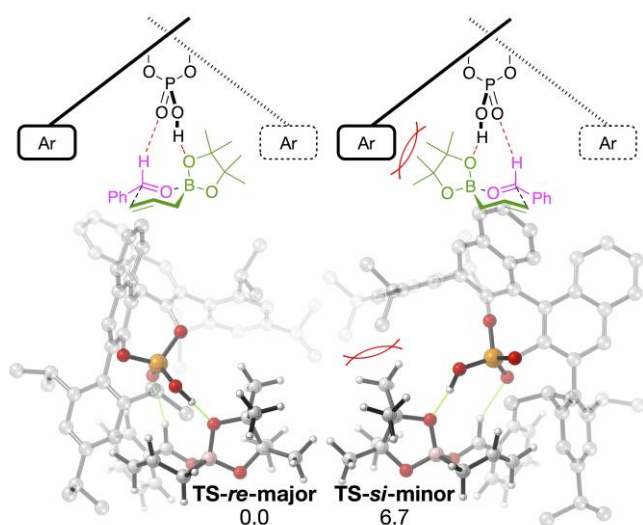


Figure 8 Goodman's stereochemical rationalization for the CPA-catalyzed enantioselective allylboration. Selectivity arises from chiral induction by the CPA anchored to the TS through hydrogen bonds. Solid green lines show electrostatic interactions, while grey lines show forming bonds. Computations performed at M06-2X/6-31G**//ONIOM (B3LYP/6-31G**::UFF), with interaction free energies given in kcal/mol.

3.3. Cooperative C(sp²)-H and C(sp³)-H donors

In complex transition states, mixed hybridizations of C–H···O interactions can and often do occur.

We reported in 2010 the mode by which proline sulfonamide catalysts effect stereocontrol in an aldol (Figure 9).⁴⁴ The sulfonamide oxygens non-classically hydrogen bond with the formyl proton of the electrophile. In addition, another sulfonamide NCHB with the cyclohexyl methylene group is only

possible in the *anti*-enamine approach of the electrophile.

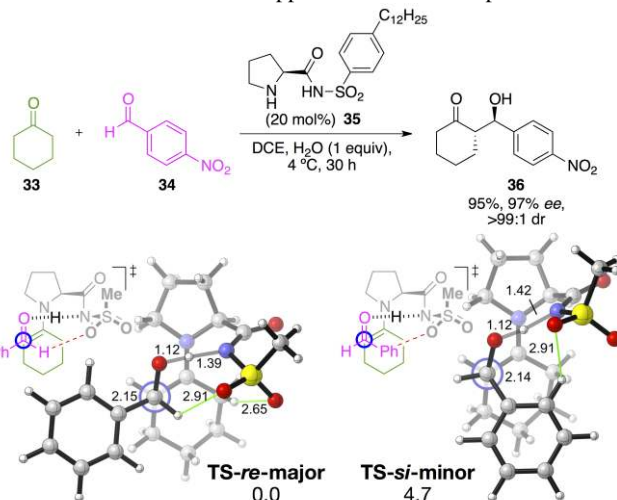


Figure 9 Proline sulfonamide-catalyzed aldol reaction. A formyl NCHB selects for the *re* face of the incoming aldehyde. Computations performed at SCS-MP2/cc-pV ∞ Z//B3LYP/6-31G*, with interaction free energies given in kcal/mol.

Planar-chiral DMAP derivative catalyst, PPY*, was known for almost two decades as a general catalyst for ketene additions. Our recent report⁴⁵ on the mechanism and stereocontrol behind planar-chiral PPY*-catalyzed pyrrole additions⁴⁶ to ketenes uncovered the importance of C(sp³)-H···O in this catalyst's general mode of ketene activation.⁴⁷ Shown in Figure 10, following nucleophilic addition of the catalyst to the ketene, the ketene enolate oxygen is sandwiched between the ferrocene rings in a cage of NCHBs formed from the top cyclopentadiene and the bottom permethylated cyclopentadiene. This both stabilizes the alkoxide and, in combination with the planar chirality of the catalyst, imparts selectivity in the subsequent nucleophilic attack by the incoming pyrrole.

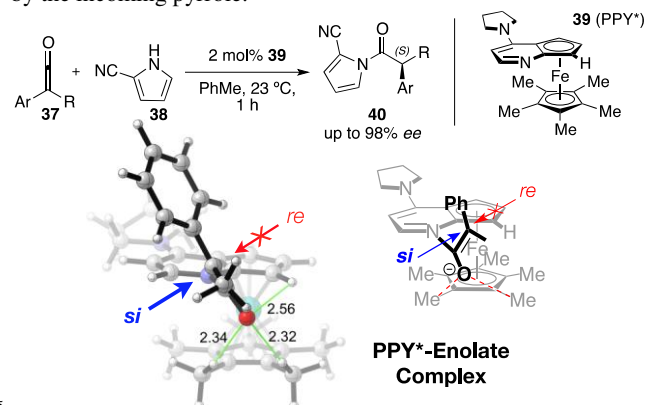


Figure 10 Planar-chiral PPY*-ketene enolate is exposed on the *si*-face. Solid green/dotted red lines show electrostatic interactions. Computations performed at SCS-MP2/def2- ∞ //B3LYP/6-31G*, with free energies given in kcal/mol.

4 Application of C–H···O Model to a New System

Full and developing negative charges in TSs can be stabilized through NCHB interactions. Methylene and methine units α to a full or developing positive charge have increased NCHB donating

ability. If a nearby developing negative charge is conformationally able to come into van der Waals proximity, stabilizing C–H...O interactions will occur. These interactions become stereocontrolling when they introduce conformational preference and rigidity in the presence of pre-existing chiral steric environment. Analyzing reactions in these terms suggest that the NCHB contributes to the stereocontrol of a wider variety and range of reactions than presently recognized in the literature.

Lu's 2011 report⁴⁸ of an enantioselective phosphinothiourea-catalyzed⁴⁹ Morita-Baylis-Hillman reaction displays many of the factors necessary for the existence of stereocontrolling C–H...O interactions (Figure 11). In the proposed transition state model, the enolate approach is controlled by classical hydrogen bonds with the thiourea moiety. However, we postulate that there is a developing negative charge on the electrophile carbonyl oxygen that is stabilized by non-classical hydrogen bonds to the hydrogens of the phosphonium α -methylene group (**48**, highlighted in blue).⁵⁰

Through classical hydrogen bonding, the thiourea moiety controls the E/Z enolate geometry; this combined with the OTBS group blocking the top face allows approach of the electrophile to the bottom face of the enolate. The geometric constraints imposed by the C(sp³)–H...O interaction controls the face of the approaching electrophile. The electrophile must approach with the *re* face, orienting the *p*-nitrophenyl group *exo* to avoid steric occlusion with the catalyst.

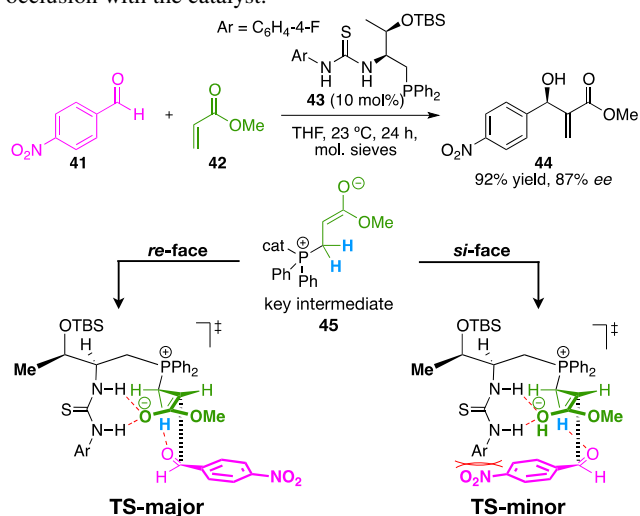


Figure 11 We propose that a critical NCHB controls the stereoselectivity of Lu's phosphinothiourea-catalyzed MBH reaction. C(sp³)–H donors highlighted in blue.

5 Conclusions

These studies provide a set of guidelines and scenarios where critical and selective stabilizing non-classical hydrogen bonding C–H...O interactions might be operative so that informed predictions may be made without the use of computations. Although transient and relatively weak, C–H...O interactions are strong enough to render complete control of selectivity in synthetic reactions. These interactions may be much more prevalent, and perhaps more commonplace in stereocontrol than currently acknowledged.

Notes and references

153 Gilbert Hall, Department of Chemistry, Oregon State University, Corvallis, OR, US. Tel: 1 541 737-2081; E-mail: paulc@science.oregonstate.edu

- (a) T. S. Moore and T. F. Winmill, *J. Chem. Soc., Trans.*, 1912, **101**, 1635–1676. (b) W. M. Latimer and W. H. Rodebush, *J. Am. Chem. Soc.*, 1920, **42**, 1419–1433.
- (a) L. Pauling, *The nature of the chemical bond and the structure of molecules and crystals: an introduction to modern structural chemistry*, Cornell University Press, 1939. (b) E. Arunan, G. R. Desiraju, R. A. Klein, J. Sadlej, S. Scheiner, I. Alkorta, D. C. Clary, R. H. Crabtree, J. J. Dannenberg, P. Hobza, H. G. Kjaergaard, A. C. Legon, B. Mennucci, and D. J. Nesbitt, *Pure Appl. Chem.*, 2011, **83**, 1619–1636.
- W. C. Hamilton and J. A. Ibers, *Hydrogen bonding in solids: methods of molecular structure determination*, W. A. Benjamin, 1968.
- G. A. Jeffrey and W. Saenger, *Hydrogen Bonding in Biological Structures*, Springer-Verlag, 1991.
- M. C. R. Symons, *Nature*, 1972, 239, 257–259.
- (a) L. Pauling and R. B. Corey, *J. Am. Chem. Soc.*, 1950, **72**, 5349–5349. (b) L. Pauling and R. B. Corey, *Proc. Natl. Acad. Sci. USA*, 1951, **37**, 235–240. (c) G. R. Desiraju, *Acc. Chem. Res.*, 1996, **29**, 441–449.
- (a) W. D. Kumler, *J. Am. Chem. Soc.*, 1935, **57**, 600–605. (b) W. J. Dulmage and W. N. Lipscomb, *Acta Cryst.*, 1951, **4**, 330–334.
- (a) D. J. Sutor, *J. Chem. Soc.*, 1963, 1105–1110. (b) R. Taylor and O. Kennard, *J. Am. Chem. Soc.*, 1982, **104**, 5063–5070. (c) S. K. Burley and G. A. Petsko, *FEBS Letters*, 1986, **203**, 139–143. (d) H. S. Rzepa, M. H. Smith, and M. L. Webb, *J. Chem. Soc., Perkin Trans. 2*, 1994, 703–707.
- E. B. Starikov and T. Steiner, *Acta Cryst.*, 1997, **D53**, 345–347.
- U. Koch and P. L. A. Popelier, *J. Phys. Chem.*, 1995, **99**, 9747–9754.
- J. E. Del Bene, *J. Chem. Phys.*, 1972, **57**, 1899–1908.
- G. G. R. Desiraju and T. Steiner, *The Weak Hydrogen Bond: In Structural Chemistry and Biology*, Oxford University Press, 1999.
- T. Steiner and G. R. Desiraju, *Chem. Comm.*, 1998, 891–892.
- (a) Y. Gu, T. Kar, and S. Scheiner, *J. Am. Chem. Soc.*, 1999, **121**, 9411–9422. (b) G. R. Desiraju, *Angew. Chem., Int. Ed.*, 2011, **50**, 52–59.
- (a) M. Alcamí, O. Mó, and M. Yáñez, *J. Phys. Org. Chem.*, 2002, **15**, 174–186. (b) T. Steiner, *Angew. Chem., Int. Ed.*, 2002, **41**, 48–76.
- (a) J. E. Del Bene, *J. Phys. Chem.*, 1988, **92**, 2874–2880. (b) S. Scheiner and T. Kar, *J. Phys. Chem. A*, 2002, **106**, 1784–1789.
- TSs are able to be observed in real time using pico- and femto-second spectroscopy; however, this is not a commonspectroscopic characterization technique utilized in many organic labs due to its high cost. For examples see: (a) N. F. Scherer, L. R. Khundkar, R. B. Bernstein, and A. H. Zewail, *J. Chem. Phys.*, 1987, **87**, 1451–1453. (b) M. Dantus, M. J. Rosker, and A. H. Zewail, *J. Chem. Phys.*, 1987, **87**, 2395–2397.
- J. Joseph and E. D. Jemmis, *J. Am. Chem. Soc.*, 2007, **129**, 4620–4632.
- S. Scheiner, S. J. Grabowski, and T. Kar, *J. Phys. Chem. A*, 2001, **105**, 10607–10612.
- (a) E. J. Corey, J. J. Rohde, A. Fischer, and M. D. Azimioara, *Tetrahedron Lett.*, 1997, **38**, 33–36. (b) E. J. Corey and J. J. Rohde, *Tetrahedron Lett.*, 1997, **38**, 37–40. (c) E. J. Corey, D. Barnes-Seeman, and T. W. Lee, *Tetrahedron Lett.*, 1997, **38**, 1699–1702. (d) E. J. Corey, D. Barnes-Seeman, and T. W.

- Lee, *Tetrahedron Lett.*, 1997, **38**, 4351–4354. (e) E. J. Corey and T. W. Lee, *Chem. Comm.*, 2001, 1321–1329.
- 21 R. Castellano, *Curr. Org. Chem.*, 2004, **8**, 845–865.
- 22 C. E. Cannizzaro and K. N. Houk, *J. Am. Chem. Soc.*, 2002, **124**, 7163–7169.
- 23 T. Kar and S. Scheiner, *J. Phys. Chem. A*, 2004, **108**, 9161–9168.
- 24 (a) H. Yang and M. W. Wong, *J. Am. Chem. Soc.*, 2013. ASAP doi: 10.1021/ja4005893. (b) N. Çelebi-Ölçüm, V. Aviyente, and K. N. Houk, *J. Org. Chem.*, 2009, **74**, 6944–6952. (c) T. C. Cook, M. B. Andrus, and D. H. Ess, *Org. Lett.*, 2012, **14**, 5836–5839. (d) G. Vayner, K. N. Houk, and Y.-K. Sun, *J. Am. Chem. Soc.*, 2004, **126**, 199–203.
- 25 (a) Z. G. Hajos and D. R. Parrish, *J. Org. Chem.*, 1974, **39**, 1615–1621. (b) U. Eder, G. Sauer, and R. Wiechert, *Angew. Chem., Int. Ed.*, 1971, **10**, 496–497.
- 26 (a) S. Bahmanyar and K. N. Houk, *J. Am. Chem. Soc.*, 2001, **123**, 12911–12912. (b) S. Bahmanyar and K. N. Houk, *Org. Lett.*, 2003, **5**, 1249–1251. (c) F. R. Clemente and K. N. Houk, *Angew. Chem., Int. Ed.*, 2004, **43**, 5766–5768. (d) P. H.-Y. Cheong, H. Zhang, R. Thayumanavan, F. Tanaka, K. N. Houk, and C. F. Barbas, *Org. Lett.*, 2006, **8**, 811–814. (e) P. H.-Y. Cheong and K. N. Houk, *Synthesis*, 2005, 1533–1537.
- 27 (a) D. Suarez, T. L. Sordo, and J. A. Sordo, *J. Am. Chem. Soc.*, 1994, **116**, 763–764. (b) D. Suarez, J. Gonzalez, T. L. Sordo, and J. A. Sordo, *J. Org. Chem.*, 1994, **59**, 8058–8064.
- 28 B. Deguin and P. Vogel, *J. Am. Chem. Soc.*, 1992, **114**, 9210–9211.
- 29 (a) J. G. Martin and R. K. Hill, *Chem. Rev.*, 1961, **61**, 537–562. (b) C. S. Wannere, A. Paul, R. Herges, K. N. Houk, H. F. Schaefer, and P. Von Ragué Schleyer, *J. Comp. Chem.*, 2007, **28**, 344–361.
- 30 I. Washington and K. N. Houk, *Angew. Chem., Int. Ed.*, 2001, **40**, 4485–4488.
- 31 (a) J. S. Brodbelt, J. Isbell, J. M. Goodman, H. V. Secor, and J. I. Seeman, *Tetrahedron Lett.*, 2001, **42**, 6949–6952. (b) J. H. Xia, B. Y. Liub, and Z. Liub, *Acta Cryst.*, 2010, **E66**, o1341.
- 32 (a) S. Arseniyadis, D. V. Yashunsky, M. M. Dorado, R. B. Alves, E. Toromanoff, L. Toupet, and P. Potier, *Tetrahedron Lett.*, 1993, **34**, 4927–4930. (b) M. Hayashi, K. Tanaka, and N. Oguni, *Tetrahedron: Asymmetry*, 1995, **6**, 1833–1836.
- 33 L. Salvatella and M. F. Ruiz-López, *J. Am. Chem. Soc.*, 1999, **121**, 10772–10780.
- 34 R. Fujiyama, K. Goh, and S. Kiyooka, *Tetrahedron Lett.*, 2005, **46**, 1211–1215.
- 35 (a) E. J. Corey, T. P. Loh, T. D. Roper, M. D. Azimioara, and M. C. Noe, *J. Am. Chem. Soc.*, 1992, **114**, 8290–8292. (b) E. J. Corey, T. Shibata, and T. W. Lee, *J. Am. Chem. Soc.*, 2002, **124**, 3808–3809. (c) D. H. Ryu and E. J. Corey, *J. Am. Chem. Soc.*, 2003, **125**, 6388–6390. (d) D. H. Ryu, T. W. Lee, and E. J. Corey, *J. Am. Chem. Soc.*, 2002, **124**, 9992–9993. (e) F.-Y. Zhang and E. J. Corey, *Org. Lett.*, 2000, **2**, 1097–1100.
- 36 M. N. Paddon-Row, C. D. Anderson, and K. N. Houk, *J. Org. Chem.*, 2009, **74**, 861–868.
- 37 I. Paterson, *Synthesis*, 1998, 639–652.
- 38 (a) R. S. Paton and J. M. Goodman, *Org. Lett.*, 2006, **8**, 4299–4302. (b) R. S. Paton and J. M. Goodman, *J. Org. Chem.*, 2008, **73**, 1253–1263.
- 39 (a) Y. Li, M. N. Paddon-Row, and K. N. Houk, *J. Am. Chem. Soc.*, 1988, **110**, 3684–3686. (b) Y. Li, M. N. Paddon-Row, and K. N. Houk, *J. Org. Chem.*, 1990, **55**, 481–493. (c) A. Bernardi, A. M. Capelli, C. Gennari, J. M. Goodman, and I. Paterson, *J. Org. Chem.*, 1990, **55**, 3576–3581.
- 40 P. Jain and J. C. Antilla, *J. Am. Chem. Soc.*, 2010, **132**, 11884–11886.
- 41 (a) V. Rauniyar and D. G. Hall, *J. Am. Chem. Soc.*, 2004, **126**, 4518–4519. (b) D. S. Barnett, P. N. Moquist, and S. E. Schaus, *Angew. Chem., Int. Ed.*, 2009, **48**, 8679–8682.
- 42 M. N. Grayson, S. C. Pellegrinet, and J. M. Goodman, *J. Am. Chem. Soc.*, 2012, **134**, 2716–2722.
- 43 P. Jain, H. Wang, K. N. Houk, and J. C. Antilla, *Angew. Chem., Int. Ed.*, 2012, **51**, 1391–1394. (b) H. Wang, P. Jain, J. C. Antilla, and K. N. Houk, *J. Org. Chem.*, 2013, **78**, 1208–1215.
- 44 (a) H. Yang, S. Mahapatra, P. H.-Y. Cheong, and R. G. Carter, *J. Org. Chem.*, 2010, **75**, 7279–7290. (b) H. Yang and R. G. Carter, *Org. Lett.*, 2010, **12**, 3108–3111.
- 45 O. Pattawong, T. J. L. Mustard, R. C. Johnston, and P. H.-Y. Cheong, *Angew. Chem., Int. Ed.*, 2013, **52**, 1420–1423.
- 46 (a) J. C. Ruble and G. C. Fu, *J. Org. Chem.*, 1996, **61**, 7230–7231. (b) B. L. Hodous and G. C. Fu, *J. Am. Chem. Soc.*, 2002, **124**, 10006–10007.
- 47 Houk has previously shown that C–H···O interactions are critical in controlling the selectivity of ketene additions. See: C. E. Cannizzaro, T. Strassner, and K. N. Houk, *J. Am. Chem. Soc.*, 2001, **123**, 2668–2669.
- 48 X. Han, Y. Wang, F. Zhong, and Y. Lu, *Org. Biomol. Chem.*, 2011, **9**, 6734–6740.
- 49 K. Yuan, H.-L. Song, Y. Hu, J.-F. Fang, and X.-Y. Wu, *Tetrahedron: Asymmetry*, 2010, **21**, 903–908.
- 50 (a) R. Robiette, V. K. Aggarwal, and J. N. Harvey, *J. Am. Chem. Soc.*, 2007, **129**, 15513–15525. (b) J. Solà, A. Riera, X. Verdager, and M. A. Maestro, *J. Am. Chem. Soc.*, 2005, **127**, 13629–13633.